Sub-Milankovitch cycles in periplatform carbonates from the early Pliocene Great Bahama Bank

Lars Reuning,[1,2] John J. G. Reijmer,[1,3] Christian Betzler,[4] Axel Timmermann,[1,5] and Silke Steph[1,6]

[1]   High-resolution bulk sediment (magnetic susceptibility and aragonite content) and $\delta^{18}O$ records from two different planktonic foraminifera species were analyzed in an early Pliocene core interval from the Straits of Florida (Ocean Drilling Program site 1006). The $\delta^{18}O$ record of the shallow-dwelling foraminifera *G. sacculifer* and the aragonite content are dominated by sub-Milankovitch variability. In contrast, magnetic susceptibility and the $\delta^{18}O$ record of the deeper-dwelling foraminifera *G. menardii* show precession cycles. The relationship between the aragonite and the paleoproxy data suggests that the export of sediment from the adjacent Great Bahama Bank was triggered directly by atmospheric processes rather than by sea level change. We propose a climate mechanism that bears similarities with the semiannual cycle component of eastern equatorial Pacific sea surface temperatures under present-day conditions.

Citation: Reuning, L., J. J. G. Reijmer, C. Betzler, A. Timmermann, and S. Steph (2006), Sub-Milankovitch cycles in periplatform carbonates from the early Pliocene Great Bahama Bank, *Paleoceanography*, *21*, PA1017, doi:10.1029/2004PA001075.

1. Introduction

[2]   It is now well established that Earth's climate varies in regular Milankovitch-scale cycles (eccentricity, obliquity and precession) driven by changes in orbital geometry and hence insolation [*Hays et al.*, 1976; *Imbrie et al.*, 1984]. Sea level variations on orbital timescales lead to cyclic deposition of sediments on carbonate platforms and in the surrounding basins [*Schlager et al.*, 1994; *Kievman*, 1998]. In the past two decades the knowledge about these cycles in carbonate platform sediments has advanced to an extent that Milankovitch cyclic signatures can be used to construct an astronomical timescale for the Mesozoic [e.g., *Preto and Hinnov*, 2003]. In addition to these well-known cycles, shorter millennial or sub-Milankovitch-scale periodicities have recently been reported from neritic carbonate successions, but their interpretation is yet controversial. The investigation of sub-Milankovitch periodicities in climate proxy time series has focused on late Pliocene through Holocene records, when the growth and decay of large Northern Hemisphere ice sheets were part of a highly variable climate system [*Hagelberg et al.*, 1994; *McIntyre and Molfino*, 1996; *Bond et al.*, 1997; *McManus et al.*, 1999; *Ortiz et al.*, 1999; *Rutherford and D'Hondt*, 2000; *Wara et al.*, 2000]. It is not clear in how far these sub-Milankovitch-scale climate variations can be used to explain sub-Milankovitch cycles in carbonate platform successions, which were mainly reported from sediments deposited under Mesozoic and Tertiary greenhouse world conditions [*Zühlke et al.*, 2003]. However, the few studies dealing with millennial-scale cycles prior to the onset of large-scale Northern Hemisphere glaciation confirm the presence of high-frequency variability during intervals of relative climate warmth [*Ortiz et al.*, 1999; *Draut et al.*, 2003; *Steenbrink et al.*, 2003; *Niemitz and Billups*, 2005]. This study will focus on semiprecession cycles, since sub-Milankovitch cycles with a period of about half a precession cycle where reported from different carbonate platform and climate proxy records. Semiprecession cycles in carbonate platforms settings have been explained by (1) a nonlinear response of the sedimentary system to climatic precession cycles [*Kroon et al.*, 2000; *Pittet et al.*, 2000] (2) a nonlinear response of the climate system to external precession forcing attributed either to alternating glaciation of the northern and the Southern Hemispheres during one precessional cycle [*Eberli*, 2000], or to the double peak in equatorial insolation caused by the alignment of perihelion with each equinox during one precession cycle [*Preto and Hinnov*, 2003]. No explanation was given how this double peak in insolation may be linked to specific physical climate mechanisms. The objective of this study is to evaluate the possible climatic origin of semiprecession variability recorded in carbonate platform sediments during a period of prolonged climate warmth. The early to middle Pliocene is the most recent period in geological time with abundant evidence for widespread warmth in the middle and high

---

[1]Leibniz-Institut für Meereswissenschaften, IFM-GEOMAR, Kiel, Germany.

[2]Now at Institute of Geology, RWTH Aachen University, Aachen, Germany.

[3]Now at Centre de Sédimentologie-Paléontologie, Université de Provence, Aix-Marseille I, Marseille, France.

[4]Department of Earth Sciences, University of Hamburg, Hamburg, Germany.

[5]Now at Department of Oceanography, University of Hawai'i at Manoa, Honolulu, Hawaii, USA.

[6]Now at Alfred Wegener Institute for Polar and Marine Research, Bremerhaven, Germany.
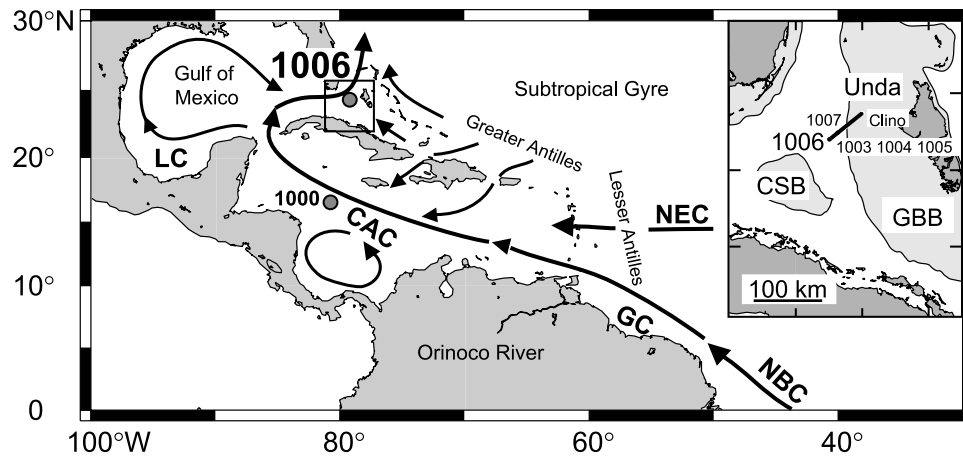
Figure 1. Modern oceanographic setting of the tropical west Atlantic showing major surface current systems. The locations of Ocean Drilling Program (ODP) sites discussed in this study are indicated. Abbreviations are NEC, North Equatorial Current; NBC, North Brazil Coastal Current; GC, Guyana Current; CAC, Caribbean Current; LC, Loop Current; CSB, Cay Sal Bank; and GBB, Great Bahama Bank. The inlet shows the location map of the Bahamas transect from the GBB to the adjacent basin of the Straits of Florida. ODP site 1006 is the most basinward site on the leeward flank of Great Bahama Bank. Position of the 100-m isobath is shown.

latitudes [*Dowsett et al.*, 1999; *Haywood et al.*, 2004]. No major ice sheets existed in the Northern Hemisphere prior to 3.5 Ma, and the amplitude of ice volume fluctuations was smaller than during the late Pliocene and Pleistocene [*Shackleton et al.*, 1995].

[3] Here we study a sediment core from Ocean Drilling Program (ODP) site 1006 situated adjacent to the Great Bahama Bank (GBB) (Figure 1). The log-derived resistivity data of the lower Pliocene interval at this site is dominated by semiprecession variability [*Kroon et al.*, 2000]. A high-resolution record of carbonate content and mineralogy was generated from ODP core 166-1006A-24H to analyze the relationship between the export of sediment from the carbonate platform and the cyclicity in the logging data. The oxygen isotopic composition of two planktonic foraminifera species, the mixed layer dweller *Globigerinoides sacculifer* and the upper thermocline dweller *Globorotalia menardii* was used to reconstruct millennial and orbital-scale variability in upper ocean hydrography. The high sedimentation rate and excellent preservation of foraminifera in the studied core offer the unique opportunity to examine paleoceanographic changes and the sensitivity of the carbonate platform at the same time and provide a detailed view into the physical mechanisms of early Pliocene tropical climate variations on millennial timescales.

2. Modern Oceanography and Climate

[4] The Florida Current (FC), which flows through the Florida Straits, is composed of two primary components; one from the wind-driven subtropical gyre and the other from the tropical South Atlantic [*Schmitz and Richardson*, 1991; *Johns et al.*, 2002]. These two water masses enter the Caribbean through several straits in the Antilles and are advected northward passing the Yucatan Channel and the Gulf of Mexico (GOM), subsequently flowing into the

Florida Straits (Figure 1). The warm relatively fresh uppermost water column of the FC is mainly of equatorial Atlantic surface water origin. In contrast, high-salinity water from the North Atlantic subtropical gyre forms the permanent upper thermocline of the FC [*Wüst*, 1964]. The transport of the FC varies on interannual and seasonal timescales. Recent estimates suggest a negative correlation between decadal variations in FC transport and the North Atlantic Oscillation (NAO) index, but the link between the two remains unclear because of the limited length of the observations [*Baringer and Larsen*, 2001]. The seasonal cycle shows an absolute transport maximum Northern Hemisphere (NH) in spring and summer and a minimum in fall [*Schott et al.*, 1988; *Molinari et al.*, 1990; *Johns et al.*, 2002]. The evolution of the seasonal cycle follows the migration of the Intertropical Convergence Zone (ITCZ) from near the equator in late winter to near 10°N in fall. From spring to summer, when the ITCZ moves northward, the water entering the southern Caribbean comes from near the equator and is transported northward in an intensified western boundary current [*Johns et al.*, 2002]. In fall, when the ITCZ is in its northernmost position a cyclonic circulation cell blocks the direct inflow of South Atlantic water to the Caribbean. At this time of the year the northward flowing South Atlantic waters are diverted offshore in the North Brazil Current Retroflection [*Johns et al.*, 2002]. The strong south easterly trade winds coupled to the northern position of the ITCZ lead to an increased mixed layer depth and hence increased heat storage in the equatorial Atlantic. When the southeast trade winds relax the ITCZ returns to its southern position near the equator and the stored heat is released to the north [*Philander and Pacanowski*, 1986].

[5] Changes in the position of the ITCZ and the associated trade wind belt also govern the seasonally varying intensity of the northeasterly trade winds, prevailing over the Bahamas and Florida Straits. During NH summer and

fall northeast trade winds weaken and precipitation rates increase over the GBB. During the boreal winter, the easterly trade winds strengthen over the GBB. During this time of the year the area is frequently affected by westerly cold fronts, which cause region-wide chilling of shelf waters and sharp water-temperature fronts within the adjacent ocean [*Wilson and Roberts*, 1995].

[6] On interannual timescales El Niño is the dominant influence on precipitation variability in the region adjacent to the GOM and Florida Straits [*Ropelewski and Halpert*, 1987]. El Niño events are associated with an amplification and equatorward shift of the subtropical Pacific Jet that brings cold fronts and rain to the region in boreal winter. During the strong El Niño 1982/1983 their occurrence was nearly doubled compared to "normal" years [*González et al.*, 2000]. During La Niña events in contrast the Pacific Jet is deflected to the north, which leads to dry and warm weather in the southern United States and the Great Plains [*Cole et al.*, 2002]. Recent results from atmospheric general circulation models suggest that on decadal timescales warmer temperatures in the EEP, similar to El Niño events, lead to increased precipitation in the Great Plains and Texas [*Schubert et al.*, 2004].

[7] Changes in the atmospheric North Atlantic Oscillation (NAO) on interannual to decadal timescales influence the winter temperature variability in the southeastern US including the GOM and Florida. The influence of the NAO on precipitation, in contrast, is weak in this region [*Marshall et al.*, 2001].

3. Material and Methods

[8] Site 1006 is situated in the Straits of Florida (24°24′N, 79°28′W), approximately 30 km from the western leeward platform edge of the GBB. The early Pliocene sediments at this site consist of nannofossil ooze from a drift deposit which interfingers in upslope direction, with prograding carbonate bank deposits from Great Bahama Bank [*Eberli et al.*, 1997].

3.1. Age Control

[9] The sedimentary sequence at hole 1006A is remarkably continuous, expanded, and precisely dated [*Eberli et al.*, 1997]. For our study we have chosen core 166-1006A-24H (216.1–225.6 mbsf), which contains two distinct cycles in the core-derived magnetic susceptibility log and lies close to the last occurrence (LO) of *Globigerina (Zeaglobigerina) nepenthes* at 240.28 mbsf [*Kroon et al.*, 2000]. Different ages of 4.18 Ma [*Berggren et al.*, 1995] and 4.39 Ma [*Chaisson and Pearson*, 1997] have been assigned to this bioevent. Since the biostratigraphy in both studies was astronomically calibrated the discrepancy could arise from taxonomic problems or diachrony. An age was assigned to the depth of the studied core by counting core-derived magnetic susceptibility cycles in up-core direction from this bioevent. Following this procedure the two magnetic susceptibility cycles in core 1006A-24H are cycle number seven and eight. Assuming a period of 22 kyr for each cycle, the studied core represents two precession cycles between 4.00 and 4.05 Ma or 4.21 and 4.26 Ma,

according to *Berggren et al.* [1995] and *Chaisson and Pearson* [1997] respectively.

[10] *Kroon et al.* [2000] demonstrate for the lower Pliocene interval (180–360 mbsf) of hole 1006A that sedimentation rates calculated from the detailed biostratigraphy agree well with the sedimentation rates calculated from the cyclic core-derived magnetic susceptibility record, assuming a precessional periodicity of 22 kyr per cycle. They note that the log-derived resistivity (SFLU) record contains regularly spaced cycles with about half the period of the core-derived magnetic susceptibility cycles and that these cycles appear to occur twice per precessional cycle. For the middle-upper Miocene section of Site 1006 a log-derived resistivity (FMS) cycle count yielded, in contrast to the lower Pliocene section, a precessional period [*Kroon et al.*, 2000].

[11] Owing to the lack of magnetostratigraphy the cyclostratigraphy could not be used to redate the biohorizons [*Kroon et al.*, 2000]. The cyclostratigraphy hence is a "floating" stratigraphy, which needs to be tied to a biostratigraphic date to yield absolute ages. In comparison to the age uncertainty arising from the biostratigraphy, other uncertainties as the exact period of the precession cycle (19 and/or 23 kyr) are minor. The simplifying assumption that the sedimentation rate is constant within each of the two magnetic susceptibility precessional cycles in core 166-1006A-24H yields a linear sedimentation rate (LSR) of ~23 cm/kyr for the upper (215.75–220.75 mbsf) and ~24 cm/kyr for the lower cycle (220.75–225.95 mbsf). The LSR for both cycles are hence very similar, but possible changes in the sedimentation rate within the individual cycles cannot be resolved. The mean sample spacing is 10 cm (minimum 8 and maximum 11 cm) for all parameters. This is equivalent to a time resolution better than 500 years, with a calculated mean resolution of 440 and 423 years for the upper and lower cycle, respectively. The sample resolution in the two cycles hence is indistinguishable given the unknown exact duration of the precession cycle (19 and/or 23 kyr). Owing to a void resulting from an interstitial water sample, no sediment sample could be taken between 218.95 mbsf and 219.16 mbsf. The missing value was interpolated from the two adjacent samples.

3.2. Methods

[12] Each sample was split in 2 sets of subsamples. One set of subsamples was homogenized in an agate mortar. The second set of subsamples was wet sieved over a 63 μm sieve to separate the sand fraction from the fine fraction.

[13] Between 5 and 10 foraminifera of the genus *Globigerinoides sacculifer* (without sac-like final end chamber) and *Globorotalia menardii* were picked from the 250–355 μm size fraction for stable isotope analysis. The shells were dissolved with 100% H_3PO_4 at 75°C in an online, automated carbonate reaction device (Kiel Device) connected to a Finnigan MAT 252 mass spectrometer. Average standard deviation based on analyses of a reference standard is <0.07‰.

[14] The total and organic carbon was measured with a Carlo Erba CHNO Analyzer NA-1500. If the results for two splits of a sample differed more than 5% from their average,
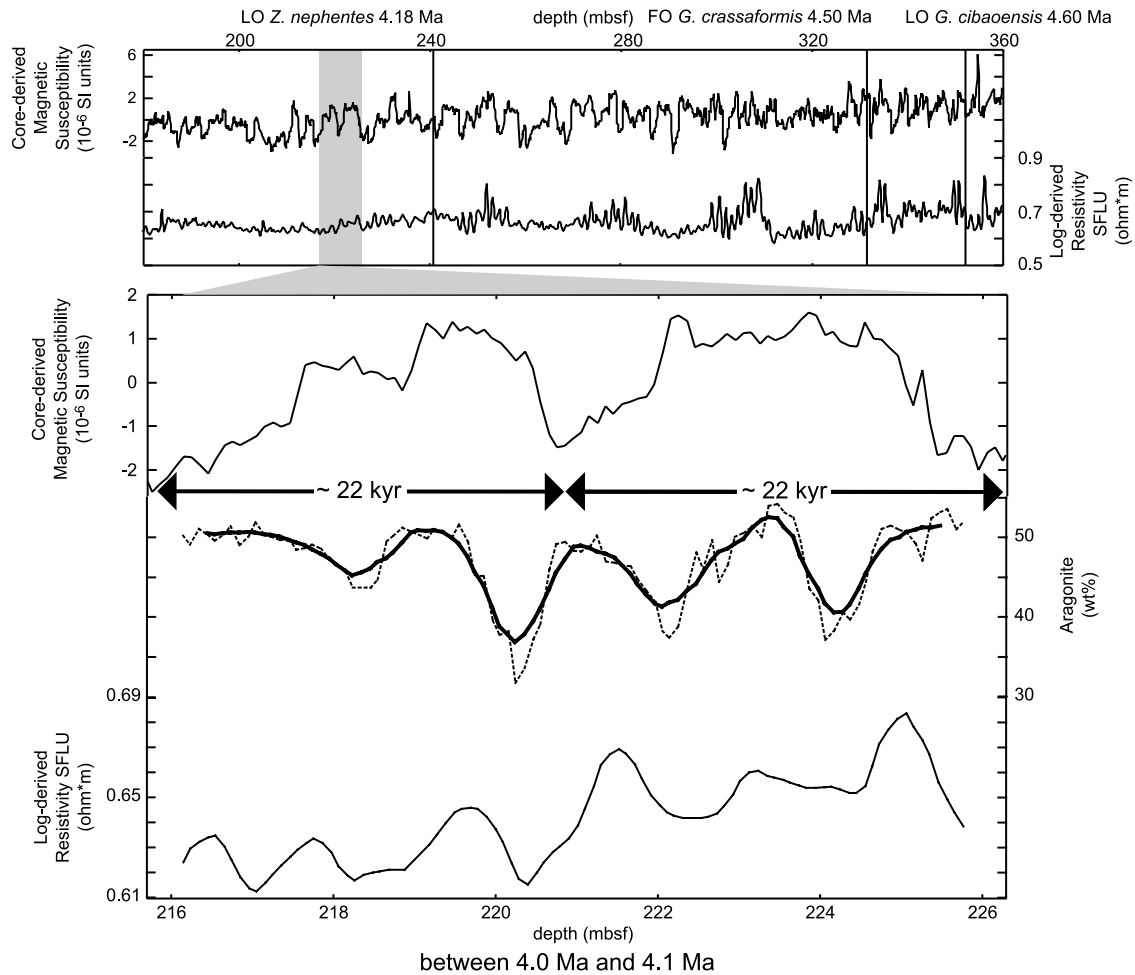
Figure 2. (top) Core-derived magnetic susceptibility and log-derived resistivity (SFLU) log of parts of sequence f. The core-derived magnetic susceptibility log is dominated by a precession signal, log-derived SFLU in contrast by a semiprecessional signal [*Kroon et al.*, 2000]. The age of the examined interval was established by counting core-derived magnetic susceptibility cycles from the nearest foraminiferal age datum. Owing to the uncertainty of this floating stratigraphy an age between 4.0 and 4.1 Ma was assigned to the two precessional cycles. (bottom) Sampled interval. The aragonite content shows a semiprecessional frequency and seems to dominate the SFLU signal. FO is first occurrence; LO is last occurrence.

the analysis was repeated. On the basis of this criterion, nine samples had to be reanalyzed. The total and organic carbon values were used to calculate the carbonate content. The standard deviation (1σ) of the carbonate content measurements of replicates is less than 2%.

[15] Carbonate mineralogy was determined using a Philips PW 1710 diffractometer with a cobalt Kα tube. Quantitative proportions of aragonite, calcite and dolomite were calculated from peak area ratios, which were measured using the computer-based integration program MacDiff (R. Petschick, MacDiff 4.1.2 Powder DiffractionSoftware, 1999, available from the author at http://www.geol.uni-erlangen.de/html/software/Macdiff.html). The standard deviation (1σ) of this method, calculated from replicates, is 1%. The absolute content of the different carbonate phases was calculated by multiplying their relative proportions with the total carbonate content. The combined error for the absolute aragonite

content is always lower than 1.5% (1σ). All analyses were carried out at IFM-GEOMAR, Kiel, Germany.

3.3. Linking Climate Proxy Records and Platform Response

[16] Apart from species-specific effects, the isotopic composition of foraminifera is determined by the temperature under which the shell is grown and the isotopic composition of the seawater. The seawater isotope content is composed of a global component, because of changes in the ice volume and a local component due to the evaporation minus precipitation balance and ocean circulation. The latter is often termed "salinity effect", since the salinity is affected by the same processes as the isotope fractionation in seawater. Here we use *G. sacculifer*, a mixed layer dweller, and *G. menardii* an upper middle thermocline dweller [*Fairbanks et al.*, 1982; *Watkins et al.*, 1998; *Schmucker*

and Schiebel, 2002] to estimate millennial-scale changes in upper ocean hydrography. The use of two species living in different water depth helps to discriminate between regional climate and ice volume fluctuations. Any ice volume effect should be present in the isotope records of both species, whereas millennial variations present in only one species can be attributed to temperature/salinity fluctuations.

[17] The mineralogy of the sediment produced on the top of carbonate platforms is dominated by aragonite. The pelagic sediment in contrast is dominated by low-Mg calcite, e.g., coccoliths and planktonic foraminifera. The aragonite content in the periplatform sediments therefore reflects the input variation from the shallow-water bank, with only minor modification by seafloor dissolution [*Schlager et al.*, 1994; *Haddad and Droxler*, 1996].

[18] A comparison of the carbonate mineralogy with the oxygen isotope signal recorded in foraminifera will hence help to understand the processes that lead to the formation of sub-Milankovitch cycles in platform development.

4. Results

4.1. Aragonite Content and Logging Data

[19] The carbonate content of the core has a mean value of 90 wt % and shows only small variations of 2.2 wt % (1σ, not shown). The total dolomite is pervasively present with a mean of <1 wt % close to the detection limit. The aragonite content varies between 32 and 54 wt % and the calcite content varies between 52 and 59 wt % (Figure 2). Relative to the length of the core-derived magnetic susceptibility cycle, which is of precessional frequency [*Kroon et al.*, 2000], the aragonite record shows pronounced shorter millennial-scale variations with amplitudes between approximately 5 and 20 wt %. Two oscillations in aragonite content occur in each core-derived magnetic susceptibility cycle, indicating a semiprecession frequency in the aragonite content. However, the lowermost and the topmost cycle are not completely documented in this core. A six-point running average was applied to the data to yield a similar "resolution" as the vertical resolution of the SFLU resistivity logging tool (~60 cm). Since the standard deviation is reduced for a mean of a number of samples following the equation: $\sigma_{total} = \sigma/N^{1/2}$, the standard deviation of the six-point running average is close to 0.6%. The aragonite content is in general positively correlated to the log-derived SFLU resistivity (Figure 2). This is most apparent for the minima in aragonite, which correspond to low log-derived resistivity values. The maxima in aragonite, in contrast, are slightly out of phase to the maxima in log-derived resistivity. A deviation from this pattern occurs at 217 mbsf, where low log-derived resistivity values are not matched by low aragonite values. Phase shifts and mismatches between logging data (resistivity) and parameters measured in the core (magnetic susceptibility, mineralogy) might result from the expansion of the cores after retrieval, possible core gaps between cores, irregularities in the shape of the borehole wall or oscillations in tool velocity up the hole. The trend of down-core increasing resistivity in the SFLU log is not reflected in the aragonite content and might be caused by narrowing of the borehole, which was recorded with the caliper log [*Eberli et al.*, 1997].
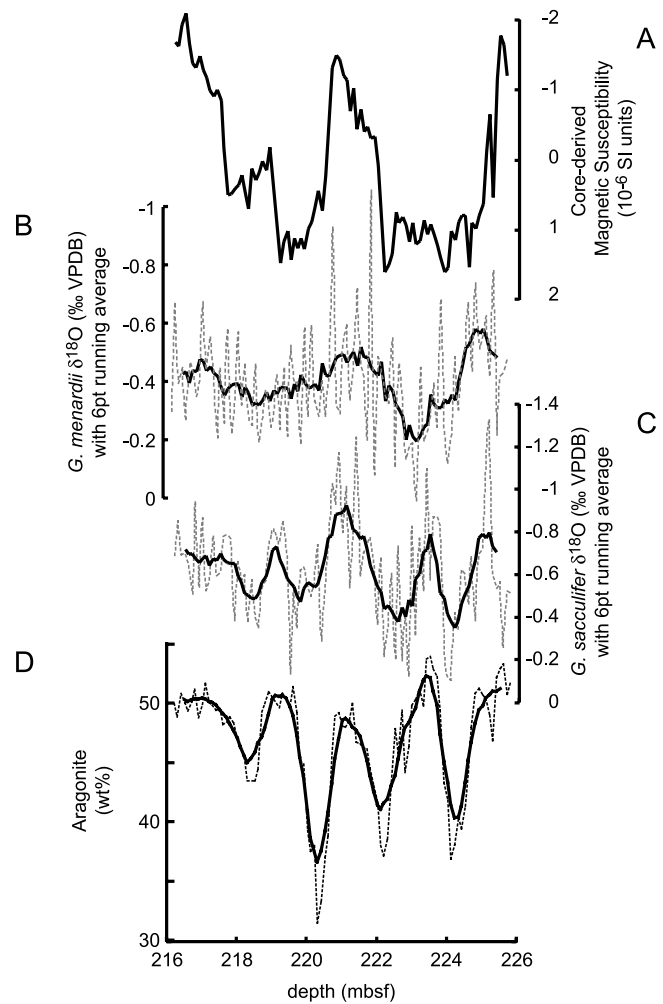

Figure 3. (a) Precession cycles in the core-derived magnetic susceptibility, plotted with reversed scale for better visualization. (b) The $\delta^{18}O$ of *G. menardii*. (c) The $\delta^{18}O$ of *G. sacculifer*. (d) Aragonite content. The bold lines are six-point running means of the raw data (dashed lines).

[20] The SFLU log is dominated by semiprecession over the entire lower Pliocene interval [*Kroon et al.*, 2000]. The apparent positive correlation between the SFLU log and the aragonite content hence suggests that semiprecession dominated the aragonite signal during the early Pliocene.

4.2. Oxygen Isotope Record

[21] The median values of $\delta^{18}O$ for *G. sacculifer* ($\delta^{18}O_{sac}$) and *G. menardii* ($\delta^{18}O_{men}$) are −0.61‰ and −0.58‰, respectively. The two $\delta^{18}O$ records show high-frequency variability of similar amplitudes superimposed upon millennial to orbital-scale changes. More than 75% of the point to point variations in both records are on the order of 0.1– 0.3‰. On timescales shorter than 1000 years, maximum variations are 0.8‰ in *G. sacculifer* and 1.0‰ in *G. menardii*. The magnitude of these variations is similar to submillennial variations described in the only other two high-resolution planktonic foraminiferal $\delta^{18}O$ records from

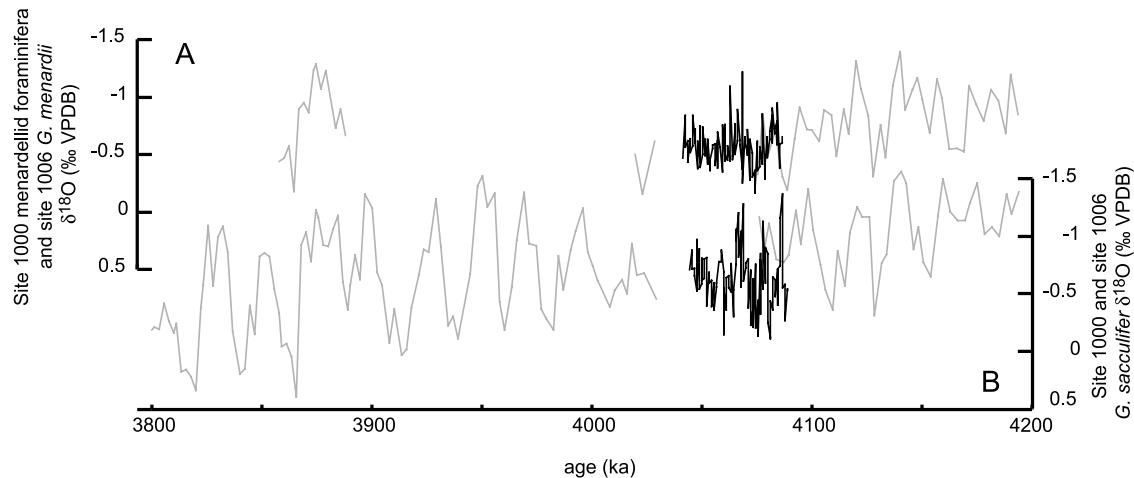**Figure 4.** Comparison of planktonic $\delta^{18}O$ records: (a) menardellid foraminifera from Caribbean site 1000 (gray [*Steph*, 2005; Steph et al., submitted manuscript, 2004]) and *G. menardii* from site 1006 (black) (this study) and (b) *G. sacculifer* from sites 1000 (gray [*Steph*, 2005]) and 1006 (black) (this study). The time interval is marked by an overall increase in planktonic $\delta^{18}O$ with strong 23-kyr cycles at site 1000. The absolute $\delta^{18}O$ values from site 1006 fit well into this trend. The $\delta^{18}O$ values of *G. menardii* at site 1006 show precession cycles, whereas the $\delta^{18}O$ values of *G. sacculifer* at site 1006 are characterized by precession and semiprecession changes (see Figure 3). The *G. sacculifer* record from site 1000 is solely dominated by precession.

the middle and early Pliocence [*Draut et al.*, 2003; *Niemitz and Billups*, 2005]. The origin of these relatively large fluctuations could reflect true high-frequency variability on interannual to centennial-timescales or result from sampling artifacts of the annual cycle, e.g., a disproportional number of foraminifera that calcified during summer or winter month in a given sample [*Lund and Curry*, 2004]. The application of a six-point running average filter reduces the effect of the latter, because of the larger amount of individuals in the grouped samples [*Lund and Curry*, 2004], and also helps to filter out variations with a period of less than ∼2500 years (∼60 cm). The very similar LSRs, inferred from the thickness of the two precessional magnetic susceptibility cycles in the core, suggest that the temporal resolution of both cycles is fairly consistent. However, changes in the aragonite content indicate some variations in the deposition rates of platform material and hence in the sedimentation rate on suborbital timescales.

[22] A comparison between the core-derived magnetic susceptibility and the filtered $\delta^{18}O_{men}$ show coherent oscillations in both records (Figure 3). The amplitudes of these oxygen isotope oscillations in the six-point running average filter are 0.2 and 0.4‰.

[23] In contrast, the filtered $\delta^{18}O_{sac}$ record shows two oscillations within each precessional magnetic susceptibility cycle. The amplitudes of these oscillations in the six-point running average filter range from 0.2 to 0.5‰. The smoothed aragonite content and the filtered $\delta^{18}O_{sac}$ are negatively correlated (Figure 3). The occurrence of a double peak of $\delta^{18}O_{sac}$ during one precessional magnetic susceptibility cycle and the covariation with the aragonite content indicate a semiprecessional period of these oscillations. The amplitudes of the millennial-scale variations in *G. sacculifer* and *G. menardii* are well above the standard deviation of the

measurement error for the six-point running average (less than 0.03‰).

5. Discussion
5.1. Precession Cycle

[24] The core-derived magnetic susceptibility record of the lower Pliocene interval in hole 1006A, which reflects the relative proportion of carbonate versus clay minerals [*Kroon et al.*, 2000], is characterized by precessional cycles. Since ODP site 1006 is surrounded by carbonate banks (Figure 1), it was suggested that the source area for the siliciclastics is Cuba [*Eberli et al.*, 1997; *Kroon et al.*, 2000]. We can rule out that cyclic dilution of siliciclastic material due to variable input of neritic material governs the core-derived magnetic susceptibility record, since the aragonite content is not anticorrelated to the magnetic susceptibility variations. Magnetic susceptibility cycles often reflect the variable input of siliciclastic minerals caused by climate change [*Ellwood et al.*, 2000]. The dominance of precessional climate variability in tropical climate is well established for the early Pliocene [*Hagelberg et al.*, 1994; *Tiedemann et al.*, 1994]. Hence we believe that low-latitude climate fluctuations linked to precessional insolation changes are the most likely candidate for the formation of the magnetic susceptibility cycles.

[25] The two precessional cycles in the smoothed $\delta^{18}O_{men}$ record have amplitudes of ∼0.2 and 0.4‰. This is equivalent to a temperature variation of $1°-2°C$ in the upper thermocline, assuming a $\delta^{18}O$:temperature relationship of ∼0.22‰/°C [*Mulitza et al.*, 2003]. Interpreted as salinity change, the $\delta^{18}O$ variability would reflect changes of ∼0.7–1.3 psu if we assume a $\delta^{18}O$:salinity relationship of 0.3 ‰ psu [*Rühlemann et al.*, 1999]. Most early Pliocene benthic

$\delta^{18}O$ records show only weak variability in the precession band. The contribution of ice volume fluctuations to the signal therefore seems to be minor [*Tiedemann et al.*, 1994; *Shackleton et al.*, 1995].

[26] Results from ocean general circulation models indicate that prior to the closing of the Isthmus of Panama three source regions contributed to the water masses in the FC: the wind-driven subtropical gyre of the North Atlantic, the equatorial South Atlantic and the tropical east Pacific [*Maier-Reimer et al.*, 1990; *Mikolajewicz and Crowley*, 1997]. Planktonic $\delta^{18}O$ records from the equatorial east Pacific (site 851) and the western equatorial Atlantic (site 925) show no or only weak responses to precessional forcing [*Cannariato and Ravelo*, 1997; *Billups et al.*, 1998]. The $\delta^{18}O$ record of planktonic foraminifera living in the mixed layer and upper thermocline at site 1000 (Figure 4) at the Nicaragua Rise in the western Caribbean [*Steph*, 2005; S. Steph et al., Changes in Caribbean surface hydrography during the Pliocene shoaling of the Central American Seaway, submitted to *Paleoceanography*, 2004, hereinafter referred to as Steph et al., submitted manuscript, 2004] in contrast shows strong variability on precessional timescales. This indicates that the precession cycle originates within the Caribbean. *Steph* [2005] suggests that these cycles represent high-amplitude salinity variations, caused by the variable inflow of low-salinity water from the eastern equatorial Pacific (EEP) to the more saline Caribbean, through the partially open Isthmus of Panama. It is extremely unlikely that these salinity fluctuations would not be advected northward through the Gulf of Mexico (GOM) into the Straits of Florida (Figure 1). Hence we interpret the precession signal in $\delta^{18}O_{men}$ and the precessional component in $\delta^{18}O_{sac}$ as the same salinity signal that was recorded at site 1000.

5.2. Semiprecession Cycle

[27] We found a pronounced semiprecessional signal in the aragonite content and the $\delta^{18}O$ signal of *G. sacculifer* in core 1006A-24H (Figure 3). The semiprecession cycles in the aragonite content correlate negatively to the $\delta^{18}O_{sac}$ record. *Kroon et al.* [2000] suggested that the semiprecession cycles represent fluctuating platform sediment shedding during rise and fall of one precessional sea level cycle. This would be an example for nonlinear recording of a climate signal by the sedimentary system. However, the $\delta^{18}O_{sac}$ record clearly shows that semiprecessional cycles at GBB are climate cycles and that the aragonite content is a quasi-linear recorder of these variations. Any ice volume effect should be present in the isotope records of both foraminifera species. The absence of a semiprecession signal in $\delta^{18}O_{men}$ provides strong evidence, that this cyclicity is not related to ice volume but to temperate/salinity fluctuations. The coherent variations in $\delta^{18}O_{sac}$ and aragonite suggest that the export of sediment from the adjacent Great Bahama Bank was triggered directly by climatic processes, rather than by sea level change.

5.3. Phase Relationships Between Precession and Semiprecession in Insolation

[28] The phase relationship between precession and semiprecession is important to unravel the underlying climatic

processes. Higher-order statistical methods have been used to determine the extent of nonlinear coupling between oscillations at Milankovitch frequencies and harmonic frequencies [*Hagelberg et al.*, 1994; *Rutherford and D'Hondt*, 2000; *Wara et al.*, 2000]. The record presented in this study is too short to statistically quantify the phase relationship between precession and semiprecession. However, the record examined has the advantage that the precession (core-derived magnetic susceptibility, $\delta^{18}O_{men}$) and the semiprecession frequency (aragonite, $\delta^{18}O_{sac}$) can be observed in different parameters measured in the same samples. The visual correlation between the *G. sacculifer* and the *G. menardii* signal seems to indicate a constant phase relationship (Figure 5). As *Rutherford and D'Hondt* [2000] pointed out, semiprecessional harmonics of precessional frequencies can be generated in two ways. For both cases the annual cycle at the equator is a useful analog. First, because the Northern and Southern Hemispheres are out of phase by 180° with respect to (season) precession, the export of a Southern Hemisphere precessional (seasonal) signal to the Northern Hemisphere will produce a semiprecession (semiannual) signal in the Northern Hemisphere when perihelion is aligned with each solstice.

[29] Second, the insolation maxima resulting from the alignment of perihelion with the spring and fall equinoxes are half a precession cycle apart at the equator [*Berger and Loutre*, 1997]. The twice yearly passage of the sun above the equator during spring and fall equinox, which produces semiannual insolation maxima, is an analog for this case.

[30] The phase relationship in the oxygen isotope records much more resembles the tropical forcing, if we assume that the maxima in the $\delta^{18}O_{men}$ precession cycle are coherent with maximum Northern Hemisphere insolation (Figure 5). This seems to be justified, since the benthic oxygen isotope stratigraphy for site 1000 indicates such a correlation for the precession cycles recorded in planktonic foraminifera at site 1000 [*Steph*, 2005; Steph et al., submitted manuscript, 2004]. The semiprecession signal of $\delta^{18}O_{sac}$ is shifted by about 90° relative to the maxima in the $\delta^{18}O_{men}$ precession signal. Hence we propose that the heavy oxygen isotope values of the semiprecession cycles represent maxima in spring and autumn insolation.

[31] The direct influence of the semiprecession component in insolation is only strong at the equator. It is therefore unlikely that the semiprecession signal at GBB results from local insolation forcing. To explain the observed semiprecessional frequency it is therefore necessary to find a teleconnections mechanism from the tropics that influences the oxygen isotope system and the aragonite sedimentation at the GBB.

[32] Semiprecessional variability in the oxygen isotope difference ($\Delta\delta^{18}O$) between *G. sacculifer* and *Neogloboquadrina dutertrei* was observed at the western tropical Atlantic site 925 during an early Pliocene time interval [*Niemitz and Billups*, 2005]. The $\Delta\delta^{18}O$ at this site is taken as the mixed layer to thermocline thermal gradient and by inference as an indicator of mixed layer depth. *Niemitz and Billups* [2005] argue that a weakening of the southeasterly trade winds at this site could be coupled to the alignment of perihelion with the spring and fall equinoxes. During the
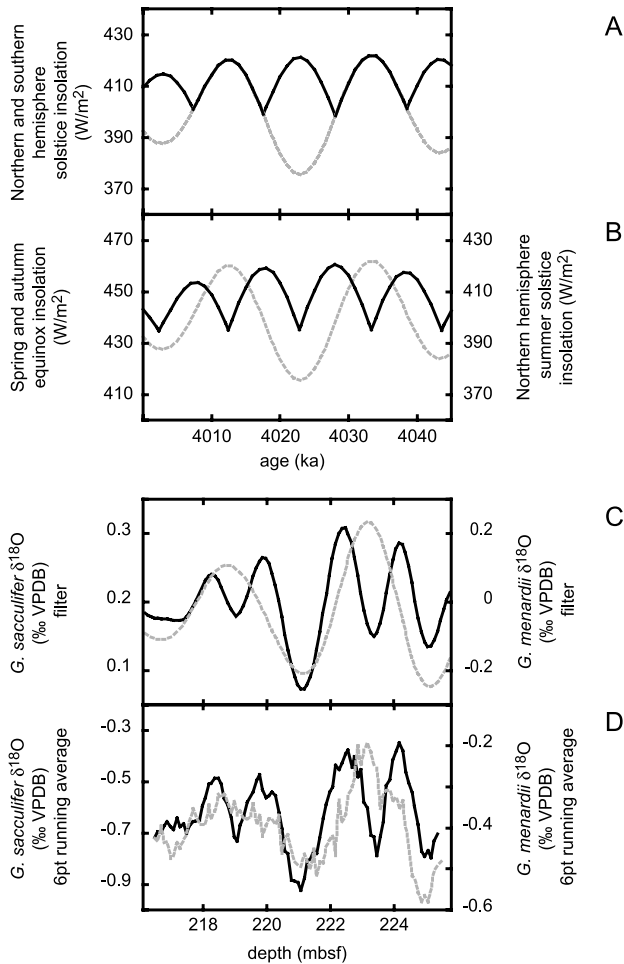
Figure 5. Comparison of the phase relationship between semiprecession and precession. (a) Largest of the two values of the daily insolation at the boreal and austral summer solstice at the equator (solid line). The remaining part of the boreal summer solstice (dashed line) is shown for visualization of the phase relationship. (b) Largest of the two values of the daily insolation at the spring and autumn (solid line) equinoxes at the equator. The boreal summer solstice (dashed line) is shown for visualization of the phase relationship. Figure 5a represents the phase relationship when a climate signal from the Southern Hemisphere is transported to the Northern Hemisphere. Figure 5b represents the phase relationship when the semiprecession forms locally close to the equator because of the alignment of perihelion with the spring and autumn equinoxes. In Figure 5a every second peak of the semiprecession cycle is 180° out of phase with respect to Northern Hemisphere insolation. In Figure 5b the semiprecession signal (solid line) is 90° out of phase with respect to Northern Hemisphere insolation (dashed line), shown here for the insolation between 4.0 Ma and 4.05 Ma [*Laskar*, 1990]. (c) Filtered $\delta^{18}O_{G.\ sac}$ raw data show a 90° out of phase relationship to the filtered $\delta^{18}O_{G.\ men}$ raw data. This is the same phase relationship as between semiprecession and precession in Figure 5b. (d) Same as Figure 5c but with a six-point running average instead of a filter.

seasonal migration of the ITCZ the weakening of the southeasterly winds leads to a reduction in mixed layer depth and to increased inflow of relatively warm and fresh water to the Caribbean and the Florida Current [*Johns et al.*, 2002]. If this mechanism holds on millennial timescales, it could explain the semiprecessional variability in the $\delta^{18}O_{sac}$ record of site 1006. At the same time the aragonite export from GBB could be influenced by long-term changes in the intensity of the northeasterly trade winds and the position of the ITCZ [*Roth and Reijmer*, 2004]. The change in trade wind strength coupled to the timing of perihelion hence could explain the coherency of the aragonite and $\delta^{18}O_{sac}$ record and their phase relationship to the precession cycle. However, the lack of a semiprecessional signal at site 1000 at the Nicaragua Rise [*Steph*, 2005; Steph et al., submitted manuscript, 2004] is in conflict with this scenario. An oceanic advection of the semiprecessional signal from site 925 to site 1006 should be recorded in the planktonic oxygen isotope record of site 1000, since the sampling resolution at this site is with <3 kyr well above the Nyquist frequency for semiprecession.

[33] Alternatively, semiprecession cycles could reflect local climate variations in the Straits of Florida brought to the region by atmospheric teleconnections. One possible candidate for such an atmospheric connection is the El Niño–Southern Oscillation (ENSO) phenomenon, originating in the eastern equatorial Pacific (EEP). Studies using ocean-atmosphere models and paleoproxy data indicate ENSO variability on semiprecessional periods [*Clement et al.*, 1999; *Turney et al.*, 2004]. Modern ENSO related temperature anomalies in the EEP have strong and stable atmospheric teleconnections to the Gulf of Mexico (GOM)/ Florida region [*Ropelewski and Halpert*, 1987; *Enfield and Mayer*, 1997; *van Oldenborgh and Burgers*, 2005]. *Molnar and Cane* [2002] find strong evidence that these teleconnections were also stable during the Pliocene. *Cronin et al.* [2002] demonstrated, based on faunal and geochemical paleosalinity proxy records, a close link between climate variability in the Pacific ocean/atmosphere system and salinity change in Florida Bay on interannual and decadal timescales. A warmer EEP (El Niño event) is associated with an amplification and equatorward shift of the subtropical Pacific Jet that brings winter storms and rain to the region. Hence we suggest that the $\delta^{18}O$ signature in surface waters originates from semiprecessional variations in fluvial runoff and local precipitation in the Florida/GOM region. The concomitant increase in aragonite export, indicated by the negative correlation of $\delta^{18}O_{sac}$ and aragonite content, could be explained by more frequent storm events. Such winter storms are an important mechanism for the export of aragonite from the modern GBB [*Pilskaln et al.*, 1989], because they bring sediment into suspension and initiate density cascading at the same time [*Wilson and Roberts*, 1995]. Thus the semiprecession signal in both the $\delta^{18}O$ *G. sacculifer* and aragonite content can be explained with atmospheric teleconnections from the EEP that are similar to modern teleconnections. Since temperature anomalies in the EEP also have a strong teleconnections to the tropical Atlantic [*Enfield and Mayer*, 1997] they could provide an alternative mechanism for the presence of semiprecession

cycles at site 925. We therefore favor the idea that the semiprecession cycles recorded at the GBB were caused by teleconnections from the EEP.

[34] The subtropical gyre is the source region for thermocline water of the Florida Current. The planktonic foraminifera species *G. menardii*, which is living in the upper thermocline, records a precessional signal at site 1006. The semiprecessional cycles therefore seem not to be caused by climate variability in the Atlantic subtropical gyre. A mechanism similar to the modern North Atlantic Oscillation also seems to be an unlikely explanation for the observed semiprecessional cyclicity at the GBB. First, the phase relationship between semiprecession and precession rather indicates a tropical origin of the signal and second, the influence of NAO on precipitation is weak in this region [*Marshall et al.*, 2001].

[35] The interpretation of the phase relationship in our record is based only on visual correlation. The significance of these observations is limited by the length of the core. We are therefore aware that the proposed mechanisms are not the only possible explanations for the observed semiprecession cycles. *Wara et al.* [2000] explained semiprecession climate variability in the North Atlantic as internal climate system variability caused by the interaction of different components of the climate system in the North Atlantic. Even though we would not expect that internal climate variability would contain the observed phase coupling between precession and semiprecession, it cannot be excluded that the coupling is a coincidence in this short interval.

5.4. Implications for the Transformation of Insolation to Climate Cycles

[36] How can semiprecession cycles in equatorial insolation be transferred to variations in SST on semiprecessional timescales in the EEP? At present semiprecessional cycles are only a minor component in the ENSO system [*Clement et al.*, 1999]. In this section we will develop a conceptual model, which demonstrates that semiprecession could have played a larger role in climate variability during the early Pliocene. To do so, we will use the semiannual insolation cycle at the equator as a modern analogue. The annual cycle in insolation dominates the SST in the largest part of the world ocean, where insolation is transferred to an annual signal in SST. However, in the equatorial Atlantic, eastern and central Pacific SST is dominated by an annual signal despite the semiannual cycle in insolation. *Xie* [1994] discussed the origin of the annual cycle in the EEP and concluded that it results from ocean-atmosphere interactions. These air-sea interactions require a shallow thermocline, like in the east Pacific, because only then the winds can readily affect SST. In the western Pacific, where the mixed layer is much deeper, the SST reflects the semiannual insolation forcing. We propose that analogous to the seasonal cycle, the semiprecessional cycle in insolation could result in an increased semiprecessional (precessional) component of maximum SSTs at the equator in the EEP, if the mean position of the thermocline is deep (shallow). The evidence for the mean position of the thermocline in the Pliocene EEP is controversial. Two different Mg/Ca-tem-

perature reconstructions for ODP site 847 in the EEP were interpreted to show either a relatively shallow position and cold SSTs [*Rickaby and Halloran*, 2005] or a deeper position and warmer SSTs [*Wara et al.*, 2005]. Mid-Pliocene alkenone-based SSTs from the same site [*Haywood et al.*, 2005] fit better to time equivalent Mg/Ca-temperature estimates of *Wara et al.* [2005]. Studies based on isotope gradients of planktonic foraminifera indicate that during the early Pliocene the thermocline in the EEP was deeper than today, with no apparent slope between the eastern and the western equatorial Pacific [*Cannariato and Ravelo*, 1997; *Chaisson and Ravelo*, 2000]. Between 4 and 4.5 Ma the thermocline shallowed progressively [*Chaisson and Ravelo*, 2000], and at least since 3 Ma it is believed to be shallow enough to enable efficient air-sea coupling in the EEP [*Philander and Fedorov*, 2003].

[37] If our analogy to the semiannual cycle were correct, a deep position of the thermocline in the early Pliocene would favor the development of semiprecession SST cycles. With a shallow thermocline in the EEP precessional changes should become stronger relative to semiprecessional variability. In addition, the response to obliquity forcing should increase in the EEP [*Philander and Fedorov*, 2003]. Planktonic $\delta^{18}O$ records from site 851 in the EEP are lacking periods at Milankovitch frequencies prior to 3.2 Ma [*Cannariato and Ravelo*, 1997]. This would be consistent with our hypothesis, if we assume a deeper early Pliocene thermocline as proposed by *Chaisson and Ravelo* [2000]. Testing our hypothesis requires the generation of high-resolution proxy time series from the EEP to confirm the presence of semiprecessional cycles in the early Pliocene.

6. Conclusion

[38] A high-resolution study of carbonate mineralogy and paleoceanographic proxies at ODP site 1006 indicates orbital and suborbital variability in the Florida Current during the Early Pliocene. The $\delta^{18}O$ record of the planktonic foraminifera *G. menardii*, living in the upper thermocline, and the core-derived magnetic susceptibility of the sediment show two precession cycles in the interval analyzed. Semiprecessional cycles are dominant in the $\delta^{18}O$ record of *G. sacculifer*, living in the surface mixed layer, and the aragonite content of the sediment.

[39] We interpret the semiprecessional cycles in $\delta^{18}O_{sac}$ and aragonite content as the result of a direct climatic influence. Semiprecessional freshwater and wind anomalies in the Caribbean appear to be captured by proxy records, such as oxygen isotopes and aragonite deposition, respectively. This hypothesis challenges the classical paradigm that attributes carbonate cycles solely to sea level variations. On the basis of an analogy to the annual cycle, we speculate that a deeper EEP thermocline in the early Pliocene facilitated the transformation of semiprecessional insolation cycle near the equator into climatic cycles.

References

Baringer, M. O., and J. C. Larsen (2001), Sixteen years of Florida Current transport at 27°N, *Geophys. Res. Lett.*, *28*, 3179–3182.

Berger, A., and M. F. Loutre (1997), Intertropical latitudes and precessional and half-precessional cycles, *Science*, *278*, 1476–1478.

Berggren, W. A., F. J. Hilgen, C. G. Langereis, D. V. Kent, J. D. Obradovich, I. Raffi, M. E. Raymo, and N. J. Shackleton (1995), Late Neogene chronology: New perspectives in high-resolution stratigraphy, *Geol. Soc. Am. Bull.*, *107*, 1272–1287.

Billups, K., A. C. Ravelo, and J. C. Zachos (1998), Early Pliocene climate: A perspective from the western equatorial Atlantic warm pool, *Paleoceanography*, *13*(5), 459–470.

Bond, W. S., W. S. Broecker, S. Johnsen, J. McManus, L. Labeyrie, J. Jouzel, and G. Bonani (1997), Correlations between climate records from North Atlantic sediments and Greenland ice, *Nature*, *365*, 143–147.

Cannariato, K. G., and A. C. Ravelo (1997), Pliocene-Pleistocene evolution of eastern tropical pacific surface water circulation and thermocline depth, *Paleoceanography*, *12*(6), 805–820.

Chaisson, W. P., and P. N. Pearson (1997), Planktonic foraminifer biostratigraphy at Site 925: Middle Miocene-Pliocene, *Proc. Ocean Drill. Program Sci. Results*, *154*, 3–31.

Chaisson, W. P., and A. C. Ravelo (2000), Pliocene development of the east-west hydrographic gradient in the equatorial Pacific, *Paleoceanography*, *15*(5), 497–505.

Clement, A. C., R. Seager, and M. A. Cane (1999), Orbital controls on the El Niño/Southern Oscillation and the tropical climate, *Paleoceanography*, *14*(4), 441–456.

Cole, J. E., J. T. Overpeck, and E. R. Cook (2002), Multiyear La Niña events and persistent drought in the contiguous United States, *Geophys. Res. Lett.*, *29*(13), 1647, doi:10.1029/2001GL013561.

Cronin, T. M., G. S. Dwyer, S. B. Schwede, C. D. Vann, and H. Dowsett (2002), Climate variability from the Florida Bay sedimentary record: Possible teleconnections to ENSO, PNA and CNP, *Clim. Res.*, *19*, 233–245.

Dowsett, H. J., J. A. Barron, R. Z. Poore, R. S. Thompson, T. M. Cronin, S. E. Ishman, and D. A. Willard (1999), Middle Pliocene paleoenvironmental reconstruction: PRISM2, *Open File Rep. 99–535*, U.S. Geol. Surv., Reston, Va.

Draut, A. E., M. E. Raymo, J. F. Mc Manus, and D. Oppo (2003), Climate stability during the Pliocene warm period, *Paleoceanography*, *18*(4), 1078, doi:10.1029/2003PA000889.

Eberli, G. P. (2000), The record of Neogene sea-level changes in the prograding carbonates along the Bahamas transect-Leg 166 synthesis, *Proc. Ocean Drill. Program Sci. Results*, *166*, 167–177.

Eberli, G. P., P. K. Swart, and M. Malone (Eds.) (1997), *Proceedings of the Ocean Drilling Program Initial Reports*, vol. 166, 850 pp., Ocean Drill. Program, College Station, Tex.

Ellwood, B. B., S. L. Benoist, R. H. Young, R. E. Crick, and A. E. Hassani (2000), Magnetosusceptibility event and cyclostratigraphy method applied to marine rocks: Detrital input versus carbonate productivity, *Geology*, *28*, 1135–1138.

Enfield, D. B., and D. A. Mayer (1997), Tropical Atlantic sea surface temperature variability and its relation to El Niño Southern Oscillation, *J. Geophys. Res.*, *102*(C1), 929–945.

Fairbanks, R. G., M. Sverdlove, R. Free, P. H. Wiebe, and A. W. H. Bé (1982), Vertical distribution and isotopic fractionation of living planktonic foraminifera from the Panama Basin, *Nature*, *298*, 841–844.

González, N. M., F. E. Müller-Karger, S. C. Estrada, R. P. de los Reyes, I. V. del Rio, P. C. Perez, and I. M. Arenal (2000), Near-surface phytoplankton distribution in the western Intra-Americas Sea: The influence of El Niño and weather events, *J. Geophys. Res.*, *105*(C6), 14,029–14,043.

Haddad, G. A., and A. W. Droxler (1996), Metastable CaCO₃ dissolution at intermediate water depth of the Caribbean and western North Atlantic: Implications for intermediate water circulation during the past 200,000 years, *Paleoceanography*, *11*(6), 701–716.

Hagelberg, T. K., G. Bond, and P. deMenocal (1994), Milankovitch band forcing of sub-Milankovitch climate variability during the Pleistocene, *Paleoceanography*, *9*(4), 545–558.

Hays, J. D., J. Imbrie, and N. J. Shackleton (1976), Variations in the Earth's orbit: Pacemaker of the ice ages, *Science*, *194*, 1121–1132.

Haywood, A. M., P. J. Valdes, and B. W. Sellwood (2004), Magnitude of climate variability during middle Pliocene warmth: A palaeoclimate modelling study, *Palaeogeogr. Palaeoclimatol. Palaeoecol.*, *188*, 1–24.

Haywood, A. M., P. Dekens, A. C. Ravelo, and M. Williams (2005), Warmer tropics during the mid-Pliocene? Evidence from alkenone paleothermometry and a fully coupled ocean-atmosphere GCM, *Geochem. Geophys. Geosyst.*, *6*(3), Q03010, doi:10.1029/2004GC000799.

Imbrie, J, J. D. Hays, D. G. Martinson, A. McIntry, A. C. Mix, J. J. Morley, N. G. Pisias, W. L. Prell, and N. J. Shackleton (1984), The orbital theory of Pleistocene climate: Support from a revised chronology of the marine δ¹⁸O record, in *Milankovitch and Climate*, edited by A. Berger, pp. 269–305, Springer, New York.

Johns, W. E., T. L. Townsend, D. M. Fratantoni, and W. D. Wilson (2002), On the Atlantic inflow to the Caribbean Sea, *Deep Sea Res., Part I*, *49*, 211–243.

Kievman, C. M. (1998), Match between late Pleistocene Great Bahama Bank and deep-sea oxygen isotope records of sea-level, *Geology*, *26*, 635–638.

Kroon, D., T. Williams, C. Pirmez, S. Spezzaferri, T. Sato, and J. D. Wright (2000), Coupled early Pliocene-middle Miocene bio-cyclostratigraphy of Site 1006 reveals orbitally induced cyclicity patterns of Great Bahama Bank carbonate production, *Proc. Ocean Drill. Program Sci. Results*, *166*, 155–166.

Laskar, J. (1990), The chaotic motion of the solar system: A numerical estimate of the size of the chaotic zones, *Icarus*, *88*, 266–291.

Lund, D. C., and W. B. Curry (2004), Late Holocene variability in Florida Current surface density: Patterns and possible causes, *Paleoceanography*, *19*, PA4001, doi:10.1029/2004PA001008.

Maier-Reimer, E., U. Mikolajewicz, and T. J. Crowley (1990), Ocean general circulation model sensitivity experiment with an open Central American Isthmus, *Paleoceanography*, *5*(3), 349–366.

Marshall, J., Y. Kushnir, D. Battisti, P. Chang, A. Czaja, R. Dickson, J. Hurrell, M. McCartney, R. Saravanan, and M. Visbeck (2001), North Atlantic climate variability: Phenomena, impacts and mechanisms, *Int. J. Climatol.*, *21*, 1863–1898.

McIntyre, A., and B. Molfino (1996), Forcing of Atlantic equatorial and subpolar millennial cycles by precession, *Science*, *274*, 1867–1870.

McManus, J. F., D. W. Oppo, and J. L. Cullen (1999), A 0.5-million-year record of millennial-scale climate variability in the North Atlantic, *Science*, *283*, 971–974.

Mikolajewicz, U., and T. J. Crowley (1997), Response of a coupled ocean/energy balance model to restricted flow through the Central American Isthmus, *Paleoceanography*, *12*(3), 429–441.

Molinari, R., E. Johns, and J. F. Festa (1990), The annual cycle of meridional heat flux in the Atlantic Ocean at 26.5°N, *J. Phys. Oceanogr.*, *20*, 476–482.

Molnar, P., and M. A. Cane (2002), El Niño's tropical climate and teleconnections as a blueprint for pre-Ice-Age climates, *Paleoceanography*, *17*(2), 1021, doi:10.1029/2001PA000663.

Mulitza, S., D. Boltovskoy, B. Donner, H. Meggers, A. Paul, and G. Wefer (2003), Temperature: δ¹⁸O relationships of planktonic foraminifera collected from surface waters, *Palaeogeogr. Palaeoclimatol. Palaeoecol.*, *202*, 143–152.

Niemitz, M. D., and K. Billups (2005), Millennial-scale variability in western tropical Atlantic surface ocean hydrography during the early Pliocene, *Mar. Micropaleontol.*, *54*, 155–166.

Ortiz, J., A. Mix, S. Harris, and S. O'Connell (1999), Diffuse spectral reflectance as a proxy for percent carbonate content in North Atlantic sediments, *Paleoceanography*, *14*(2), 171–186.

Philander, S. G. H., and A. V. Fedorov (2003), Role of tropics in changing the response to Milankovitch forcing some three million years ago, *Paleoceanography*, *18*(2), 1045, doi:10.1029/2002PA000837.

Philander, S. G. H., and R. C. Pacanowski (1986), A model of the seasonal cycle of the tropical Atlantic Ocean, *J. Geophys. Res.*, *91*, 14,192–14,206.

Pilskaln, C. H., A. C. Neumann, and J. M. Bane (1989), Periplatform carbonate flux in the northern Bahamas, *Deep Sea Res., Part A*, *36*, 1391–1406.

Pittet, B., A. Strasser, and E. Mattioli (2000), Depositional sequences in the deep-shelf environments: A response to sea-level changes and shallow-platform carbonate productivity (Oxfordian, Germany and Spain), *J. Sediment. Res.*, *70*, 392–407.

Preto, N., and L. A. Hinnov (2003), Unraveling the origin of carbonate platform cyclothems in the upper Triassic Dürrenstein formation (Dolomites, Italy), *J. Sediment. Res.*, *73*, 774–789.

Rickaby, R. E. M., and P. Halloran (2005), Cool La Niña during the warmth of the Pliocene?, *Science*, *307*, 1948–1952.

Ropelewski, C. F., and M. S. Halpert (1987), Global and regional scale precipitation patterns associated with the El Niño/Southern Oscillation, *Mon. Weather Rev.*, *115*, 1606–1626.

Roth, S., and J. J. G. Reijmer (2004), Holocene Atlantic climate variations deduced from carbonate periplatform sediments (leeward margin, Great Bahama Bank), *Paleoceanography*, *19*, PA1003, doi:10.1029/2003PA000885.

Rühlemann, C., S. Mulitza, P. J. Müller, G. Wefer, and R. Zahn (1999), Warming of the tropical Atlantic Ocean and slowdown of thermohaline circulation during the last deglaciation, *Nature*, *402*, 511–514.

Rutherford, S., and S. D'Hondt (2000), Early onset and tropical forcing of 100,000-year Pleistocene glacial cycles, *Nature*, *408*, 72–75.

Schlager, W., J. J. G. Reijmer, and A. W. Droxler (1994), Highstand shedding of carbonate platforms, *J. Sediment. Res., Sect. B*, *64*, 270–281.

Schmitz, W. J., and P. L. Richardson (1991), On the sources of the Florida Current, *Deep Sea Res.*, *38*, suppl. 1, 379–409.

Schmucker, B., and R. Schiebel (2002), Planktonic foraminifers and hydrography of the eastern and northern Caribbean Sea, *Mar. Micropaleontol.*, *46*, 387–403.

Schott, F. A., T. N. Lee, and R. Zantopp (1988), Variability of structure and transport of the Florida Current in the period range of days to seasonal, *J. Phys. Oceanogr.*, *18*, 1209–1230.

Schubert, S. D., M. J. Suarez, P. J. Pegion, R. D. Koster, and J. T. Bacmeister (2004), On the cause of the 1930s Dust Bowl, *Science*, *303*, 1855–1859.

Shackleton, N. J., M. A. Hall, and P. D. Pate (1995), Pliocene stable isotope stratigraphy of Site 846, *Proc. Ocean Drill. Program Sci. Results*, *138*, 337–355.

Steenbrink, J., M. L. Kloosterboer-van Hoeve, and F. J. Hilgen (2003), Millennial-scale climate variations recorded in early Pliocene colour reflectance time series from the lacustrine Ptolemais Basin (NW Greece), *Global Planet. Change*, *36*, 47–75.

Steph, S. (2005), Pliocene stratigraphy and the impact of Panama uplift on changes in Caribbean and tropical east Pacific upper ocean stratification (6–2.5 Ma), Ph.D. thesis, 158 pp., Univ. of Kiel, Kiel, Germany.

Tiedemann, R., M. Sarnthein, and N. J. Shackleton (1994), Astronomic timescale for the Pliocene Atlantic $\delta^{18}O$ and dust flux records of Ocean Drilling Program Site 659, *Paleoceanography*, *9*(4), 619–638.

Turney, C. S. M., A. P. Kershaw, S. C. Clemens, N. Branch, P. T. Moss, and L. K. Fifield (2004), Millennial and orbital variations of El Niño/Southern Oscillation and high-latitude climate in the last glacial period, *Nature*, *428*, 306–310.

van Oldenborgh, G. J., and G. Burgers (2005), Searching for decadal variations in ENSO precipitation teleconnections, *Geophys. Res. Lett.*, *32*, L15701, doi:10.1029/2005GL023110.

Wara, M. W., A. C. Ravelo, and J. S. Ravenaugh (2000), The pacemaker always rings twice, *Paleoceanography*, *15*(6), 616–624.

Wara, M. W., A. C. Ravelo, and M. L. Delaney (2005), Permanent El Niño-like conditions during the Pliocene warm period, *Science*, *309*, 758–761.

Watkins, J. M., A. C. Mix, and J. Wilson (1998), Living planktic foraminifera in the central tropical Pacific Ocean: Articulating the equatorial "cold tongue" during La Niña, 1992, *Mar. Micropaleontol.*, *33*, 157–174.

Wilson, P. A., and H. H. Roberts (1995), Density cascading: Off-shelf sediment transport, evidence and implications, Bahama Banks, *J. Sediment. Res., Sect. A*, *65*, 45–56.

Wüst, G. (1964), Spreading and mixing of the water types with an oceanographic atlas, in *Stratification and Circulation of the Antillean-Caribbean Basin*, 201 pp., Columbia Univ. Press, New York.

Xie, S.-P. (1994), On the genesis of the equatorial annual cycle, *J. Clim.*, *7*, 2008–2013.

Zühlke, R., T. Bechstädt, and R. Mundil (2003), Sub-Milankovitch and Milankovitch forcing on a model Mesozoic carbonate platform—The Latemar (Middle Triassic, Italy), *Terra Nova*, *15*, 69–80.

C. Betzler, Department of Earth Sciences, University of Hamburg, Hamburg D-20146, Germany.

J. J. G. Reijmer, Centre de Sédimentologie-Paléontologie, Université de Provence (Aix-Marseille I), 3 Place Victor Hugo, Case 67, F-13331 Marseille Cédex 3, France.

L. Reuning, Institute of Geology, RWTH Aachen University, Wüllnerstraß 2, D-52062 Aachen, Germany. (reuning@geol.rwth-aachen-de)

S. Steph, Alfred Wegener Institute for Polar and Marine Research, D-27515 Bremerhaven, Germany.

A. Timmermann, Department of Oceanography, University of Hawai'i at Manoa, Honolulu, HI 96822, USA.